UKACC International Conference on Control 2012
Cardiff, UK, 3-5 September 2012

Tensegrity-Based Formation Control of Unmanned Vehicles

Sook Yen Lau* and Wasif Naeem†
School of Electronics, Electrical Engineering and Computer Science
Queen's University Belfast, University Road, Belfast BT7 1NN, UK.
Email: slau02@qub.ac.uk*, w.naeem@qub.ac.uk†

***Abstract*—A new formation control methodology modelled by a virtual tendon-driven system using the tensegrity structures is presented. The objective of the work is to regulate the formation of unmanned vehicles within the communications bandwidth and perform point-to-point manoeuvring tasks. The reaction control forces that are experienced by vehicles in the formation are determined by the admissible tendon forces in tensegrity. A control law is designed to stabilize the interspacing between the vehicles in the presence of disturbances by making the combined use of string and spring characteristics. Simulation results demonstrate the effectiveness of the proposed approach in terms of maintaining the formation and avoiding inter-vehicle collisions. Formation shape changing is also performed by varying the relative parameters between the vehicles.**

I. Introduction

Formation control is a matter of controlling the relative position and orientation of an ensemble of autonomous vehicles while allowing the group to move as a whole in a stable configuration. It is proven that moving a group of vehicles is more beneficial than a single vehicle in the presence of uncertain and adverse environments. This is because vehicles in formation are able to acquire enough and accurate information from the environment, whilst enhancing their power to withstand danger. Hence, the use of groups of multiple autonomous vehicles to perform co-ordinated and co-operative tasks has been attracting a growing amount of attention recently in the area of autonomous robotics and control communities.

It is also well known that formation systems have many advantages such as wide area sensing coverage and system energy conservation due to the reduction of friction in each vehicle. Robustness and efficiency of the system also increases while offering redundancy, reconfiguration ability and structural flexibility for the system. These advantages have led formation control perform a wide variety of functions in land, marine and aerial applications. Specific applications include exploration, search and rescue, microsatellite clusters and transportation of large and heavy objects [1].

Problems to set up in co-operative formation control often involve achieving formation, maintaining formation and dynamic switching between different formation shapes whilst carrying out a task. A number of methodologies have been developed to address the shape dynamics of a group of vehicles in a plane such as implicit polynomial (IP) [2], elliptic Fourier descriptors (EFD) [2], sliding mode controllers [3], extended Kalman filter with an input-state feedback control law [4], Lyapunov function [5], to name a few.

In this paper, formation dynamics of a group of vehicles is synthesised and analysed using a virtual tendon-driven tensegrity system. Tensegrity structures are spatial structural systems with interconnected strings and bars/struts [6], where strings are the tendon members and bars/struts are the compressive members. In literature, tensegrity structures have been mainly used to design mechanical structures and little attention has been paid to their usability to develop formation control algorithms for dynamic systems. In [7], for instance, the authors have demonstrated formation for a group of vehicles using an energy-momentum method in tensegrity models. However, they assumed zero external (disturbance) forces which simplified the problem.

The new control law here is formulated to drive a dynamic group of vehicles into a specified formation with control forces that are represented by admissible tendon forces in tensegrity structures. This control law is designed to prevent strings slacking and yielding and make the structure responsive to the environment disturbance forces. In control terms, this force precludes any two vehicles coming too close to each other (string slacking) in order to avoid collision. The controller also prevents the vehicles moving too far apart from each other (string yielding) in order to keep the vehicles within the communications range. The proposed overall formation system is characterised by three main considerations: vehicles formation geometry which is modelled using the concept of tensegrity, communications topology which is represented by strings and bars of the tensegrity structure, and the interaction control algorithm.

In the remainder of this paper, Section II outlines the benefits of tensegrity properties. Formation shape and its communication topology will be described in Section III whilst tendon controller design and formation system regulation will be explained in Section IV and V respectively. Simulation results are shown in Section VI to demonstrate formation achieving, formation maintaining, formation changing and manoeuvring tasks. Concluding remarks are made in Section VII.

II. Tensegrity Structures

The artist Kenneth Snelson built the first tensegrity structure [8] and the term tensegrity was coined by Fuller as a

978-1-4673-1558-6/12/$31.00 ©2012 IEEE

contraction of tensional integrity [9]. In nature, bones and tendons of animals and humans are connected in a way that allows for smooth control movements, where the bones provide compressive load-carrying capacity while tendons provide tensions stabilizing the configuration [6]. In structural engineering, controlled tensegrity make buildings responsive to natural environmental disturbances such as earthquakes and winds [6].

In the tensegrity framework, the stability and rigidity of tensegrity structures have been proven using the model of energy function [10]. This has motivated the development of mathematical machinery in the design and analysis of static and dynamic tensegrity systems to achieve shape formation control and other engineering functions. It is possible to form a tensegrity structure by using models of springs, strings and bars which can be combined to provide greater flexibility and control of the whole unit. The extreme shape-changing ability of tensegrity structures has been proven in the approach of a robotic tensegrity worm crawls (which requires stiffness control) while squeezing through crevices requiring large shape changes [11].

In a dynamic tensegrity-based formation control, one way of controlling the position of each vehicle in the group is by varying the length of the bars. However, for simplicity, the formation controller is designed here based on the relative distance and orientation between the leader and follower vehicles. For example, if the requirement is to expand the formation, the bar lengths could be increased. The same result can also be achieved by varying the interspacing between a designated pair of vehicles by controlling the admissible tendon forces in a tensegrity structure. This tendon controller is designed by assuming a spring with elastic characteristic (non-Hookean) which experiences the properties of both spring and string.

A. Elastic Spring as Tendon

A linear spring can store energy either by applied compressive force or tensile force on it, however, a string (elastic band) can only store energy in the presence of a tensile force. In a tensegrity system, the tendon/string is always kept in tension, therefore it behaves in a similar manner to the spring. Hooke's Law states that the force that is exerted on a spring is proportional to the extension of the spring. Note that the stress and strain are (uniquely) related to force and extension of the spring, hence, the gradient of a stress - strain graph as shown in Figure 1a is identical to the force versus extension graph. However, a string with elastic characteristics, has a non-linear gradient graph as shown in Figure 1b. This property of the elastic spring is exploited in this paper and is further elaborated in Section IV on formation controller modelling.

III. Problem Formulation

An example of a 4-vehicle formation connected using the concept of tensegrity is shown in Figure 2. Here, nodes are defined as vehicles and edges are represented by strings/elastic

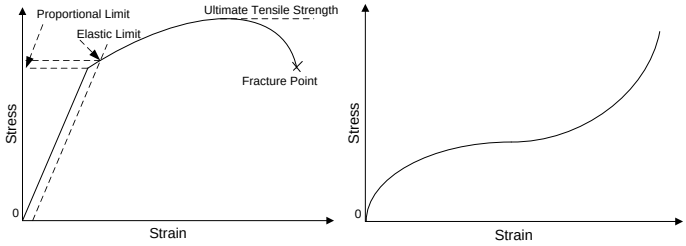

(a) Spring (b) Elastomer

Figure 1: The gradient of stress strain curves

springs(s) and bars(b). The edges correspond to communication topology and control force directions between the vehicles. A chain communication topology is assumed where each vehicle moves according to its neighbour/leader in the formation which may not be its nearest. As shown in Figure 2, UV_1 is the leader of UV_2 while UV_2 act as the leader for UV_3 and so on. $\mathbf{f}_{LF}$ represents the force that is exerted on follower (F) according to its leader (L). The magnitude of this control force is dependant on stress, ω, which is a tensegrity parameter. The edge is a string if $\omega > 0$, and is a bar if $\omega < 0$ [10]. In addition, a centralised control architecture is considered where a virtual leader (UV_1) is assigned for leading the whole formation and combined with the chain topology. Hence, the force, $\mathbf{f}_{41}$ and its corresponding communications link in Figure 2 can be ignored.

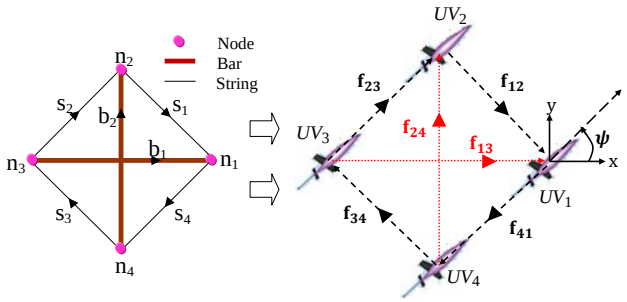

Figure 2: Vehicles communication topology referred to a C2T4 tensegrity system

It has been proven that shape changing task will be simpler to achieve by relaxing the equilibrium of the structure rather than pressing against a fixed equilibrium [6]. The tensegrity control parameter, ω will affect the edge's tension and cause another new equilibrium interspacing between the nodes. In formation control, the equilibrium interspacing between the vehicles is dependant on ω and can be represented by a virtual tendon-driven system (spring-mass system) as shown in Figure 3.

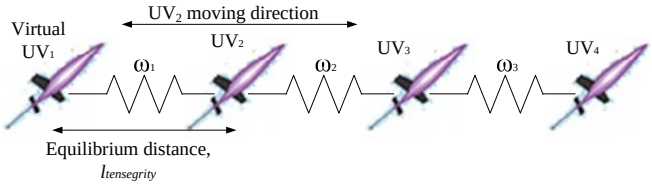

Figure 3: Formation in a virtual tendon system

The force and position of each vehicle in the tendon-driven system can be mathematically defined as

$$m\ddot{\mathbf{q}} + b\dot{\mathbf{q}} + \omega\mathbf{q} + \mathbf{f}(t) = 0 \tag{1}$$

where m is the mass of the vehicle, b is the friction coefficient and $\mathbf{q}$ is the position vector of the vehicle defining its local coordinates. ω is the sum of the two stresses $(\omega_1 + \omega_2)$ for vehicle UV_2; $(\omega_2 + \omega_3)$ for vehicle UV_3 and (ω_3) for vehicle UV_4. $\mathbf{f}(t)$ represents the applied force to the tendon system to maintain the interspacing between the vehicles. In order to compensate for uncertain environments, the plant is rewritten as

$$m\ddot{\mathbf{q}} + b\dot{\mathbf{q}} + \omega\mathbf{q} + \mathbf{f}(t) + \mathbf{d}_f = 0 \tag{2}$$

where $\mathbf{d}_f$ is an external disturbance force (e.g. wind for aircraft or current for ship). Note that the benefit of this parallel connected formation is that it is easy to keep track of every vehicle in the group. However, a major disadvantage is the error propagation from one pair of vehicles to the other.

IV. Tendon Controller Modelling

In the formation control framework, there will be $r = n-1$ communication links in a formation containing n vehicles. A separate controller is designed to control each pair of vehicles that are connected by a direct communication link. The signal measured by the controller is the relative distance between leader and follower vehicles and is denoted as l_{LF}. The controller output, $\mathbf{f}_{LF}$ is the force function which is modelled by an elastic spring. This tendon force, $\mathbf{f}_{LF}$ that is exerted on the follower vehicle with respect to its leader was designed to have a much larger elastic limit compared to its proportionality limit and is defined mathematically in Equation 3. This equation is essentially a combination of stress-strain relationship of spring and string as illustrated in Figure 1.

$$\mathbf{f}_{LF} = \begin{cases} K \ln \frac{l_{LF}}{l_{tensegrity}}(\mathbf{q}_F - \mathbf{q}_L) & \text{if } 0 < l_{LF} \leq l_{ultimate} \\ K \exp(-\frac{l_{LF} - l_{tensegrity}}{l_{break}})(\mathbf{q}_F - \mathbf{q}_L) & \text{if } l_{ultimate} < l_{LF} \leq l_{break} \\ 0 & \text{if } l_{LF} > l_{break} \end{cases} \tag{3}$$

$$K = K_1 \alpha_{LF} \omega_{LF} \tag{4}$$

Where K_1 is a gain parameter that is proportional to the disturbance force, $\mathbf{d}_f$ and helps to adapt the controller to external disturbances.

$$K_1 \propto \mathbf{d}_f \tag{5}$$

ω_{LF} represents the stress and α_{LF} is a signed scalar parameter that determines the attracting $(\alpha_{LF} > 0)$ or repelling $(\alpha_{LF} < 0)$ force that is exerted on the follower vehicle. This is further elaborated in Section IV A.

The parameter, $l_{tensegrity}$ is the desired distance between a given pair of vehicles. $l_{ultimate}$ is the maximum distance between the controlled pair of vehicles, where ultimate tensile strength (attracting or positive force) that is applied to the follower vehicle increases. After this point, this attracting force starts to reduce. This is done in order to reduce the rebound force that will occur on the follower if the disturbance is suddenly removed.

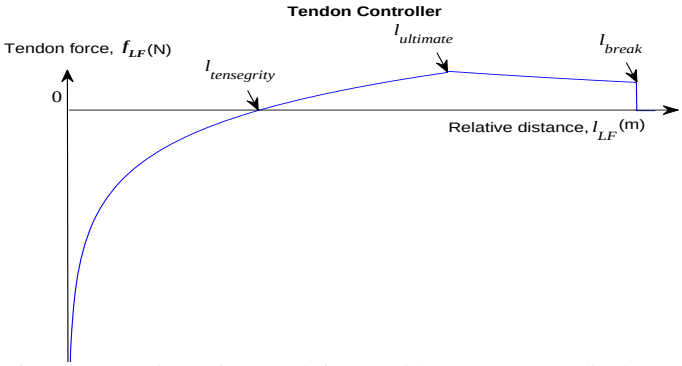

Figure 4: Design of control force with response to displacement

l_{break} is the maximum length of the string; the string is fractured at this point if the disturbance force continues to be added to the string. In formation control terms, l_{break} is the maximum communication length between the vehicles. The control force, $\mathbf{f}_{LF}$, is equal to zero at this point to give up a straying vehicle rather than trying to apply more force on it to pull it back to the formation. This vehicle might collide with the other vehicles in the formation when the disturbance force is suddenly removed due to the large restoring force.

Figure 5 is drawn to show the block diagram representation of the overall tensegrity-based nonlinear tendon-driven control for a pair of vehicles. To ensure zero steady-state tracking error, an integral term is added to the closed loop system.

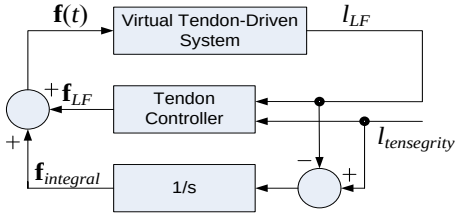

Figure 5: Block diagram of tendon-driven system with integral action

A. Analysis of Tendon Force

Tension along the spacing edge between any two vehicles is changed according to the edge's extension and can be divided into two categories: attracting force (positive force) and repelling force (negative force). By considering the two vehicles within the $l_{ultimate}$ communication range, the tendon force can be mathematically defined as in Equation 6 with the parameter K_1 set to unity for simplicity.

$$\mathbf{f}_{LF} = \alpha_{LF}\omega_{LF}[\ln l_{LF} - \ln l_{tensegrity}](\mathbf{q}_F - \mathbf{q}_L) \tag{6}$$

The equilibrium of the tendon-driven system can be found by equating the sum of all the forces that are acting on vehicles in the system to zero i.e.

$$\sum_{r=1}^{n-1} \alpha_{L_rF_r}\omega_{L_rF_r}[\ln l_{L_rF_r} - \ln l_{tensegrity_r}](\mathbf{q}_{F_r} - \mathbf{q}_{L_r}) = 0 \tag{7}$$

The subscript r refers to a particular communication link that connected a pair of vehicles and n is the total number of vehicles in the formation. Let the position vector $\mathbf{q}^e = (x^e, y^e)$ represents the equilibrium tensegrity structure. Hence, the equilibrium stress constant of a pair of vehicles can be defined as

$$\widetilde{\omega}_{LF}(x^e, y^e) = \alpha_{LF}\omega_{LF}[\ln l_{LF} - \ln l_{tensegrity}] \tag{8}$$

The edge here is modelled as a string, hence, $\omega_{LF} > 0$. Also, by assuming the tendon-driven system in equilibrium, $\widetilde{\omega}_{LF}(x^e, y^e) = \omega_{LF}$, therefore equation 8 can be simplified as

$$1 = \alpha_{LF}[\ln l_{LF} - \ln l_{tensegrity}] \tag{9}$$

Equation 9 proves that the tendon-driven system experiences an attracting force ($\alpha_{LF} > 0$) when the relative distance (l_{LF}) between the vehicles is larger than its equilibrium distance ($l_{tensegrity}$); and repelling force ($\alpha_{LF} < 0$) when the relative distance (l_{LF}) between the vehicles is smaller than its equilibrium distance ($l_{tensegrity}$).

V. Regulation of Formation Subsystem

The objective in this section is to regulate the interspacing distance between a pair of leader and follower vehicles. The equilibrium distance, $l_{tensegrity}$ and the maximum communication range, l_{break} are the key control parameters which are assumed to be 16m and 32m, respectively for simulations purposes. The two vehicles formation was simulated in a tendon-driven system using the proposed tendon controller and compared with a linear PI controller. All the parameters in tendon-driven system shown in Equation 2 are considered to be unity. And the parameters of PI controller were optimized using the Ziegler-Nichols (ZN) tuning method in order to give a fast and smooth response. The values estimated for K_P and K_I were 0.4091 and 0.1002, respectively.

Figure 6 shows that the tendon control system with a desired step response of 16m was achieved in a settling time of 50.04s with an overshoot of 1.35%, while the linear controller has a slower settling time of 60.77s and experienced a higher overshoot of 3.56%. The dip at the beginning of step response is due to the higher repelling force that was produced by the linear controller as shown in Figure 7. This repelling force was encountered because the initial spacing between the vehicles was kept very small. However, the tendon controller was able to eliminate this effect and provided a smooth and quick response to the system with a lower repelling force.

Next external disturbance forces, $\mathbf{d}_f$ of magnitude 30N and 110N were added to the subsystem to demonstrate controller performance. These impulse disturbances were triggered at 150s for a period of 150s to force change l_{LF}. Both positive and negative disturbances are considered demonstrating the dilation and squeezing of inter-vehicle spacing respectively.

Simulation results in Figure 8 depicts that an increasing positive disturbance force caused the follower and leader vehicles to further repel from each other. It can be observed that as long as the follower vehicle moves within the prescribed

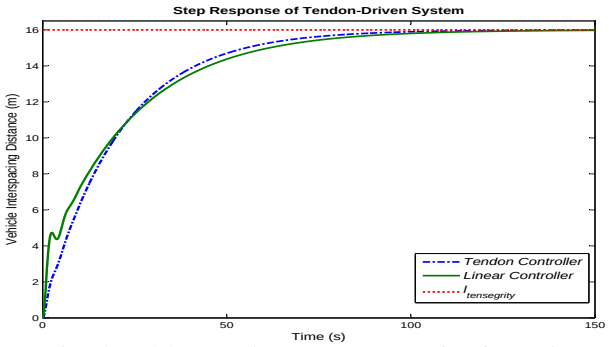

Figure 6: Closed-loop unit step response for formation subsystem

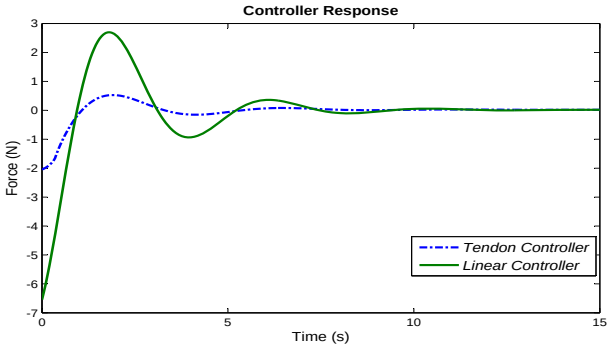

Figure 7: Subsystem controller response

communications range, the formation can be maintained (Figure 8(a)). The follower vehicle will lose communication with its leader when the separation between the vehicles is more than l_{break}, 32m. This will cause the removal of control force in order to give up the straying follower (Figure 8(b)). However, the PI controller produced a large attracting control force to the follower vehicle when it moved out of the communication to pull it back to its equilibrium position. This had caused a collision between the two vehicles when the disturbance force is suddenly removed. This collision happened due to the rebound force being larger than the vehicle's repelling force.

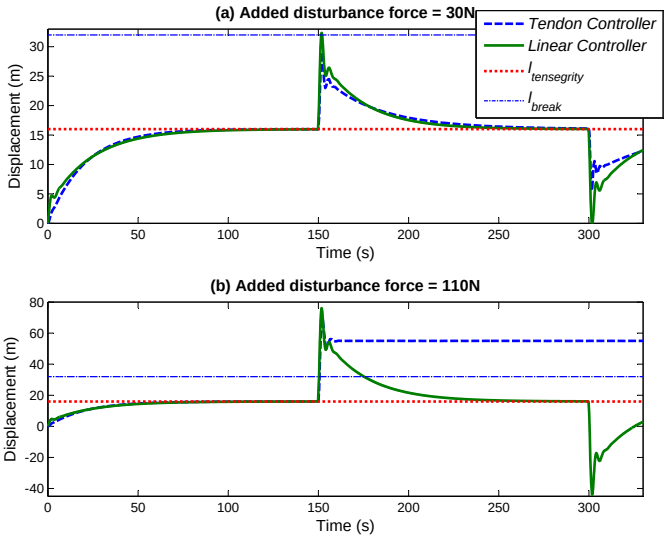

Figure 8: Step responses under positive disturbance force

Table I provides a quantitative comparison between step

responses under the positive and negative disturbance forces. In contrast to the positive disturbance force, an increasing negative disturbance force caused the distance between the two vehicles become smaller. Note that the relative distance in tendon control system is never equal to or less than zero due to the force that is exerted on the follower vehicle tends to be infinitely large (see Equation 3). This helps to prevent the collision between the vehicles. However, the linear controller was unable to prevent the collision, shown by negative bold displacement in Table I.

TABLE I: Tendon and linear controller comparison

Disturbance force $\mathbf{d}_f$, (N)	maximum and minimum vehicles interspacing (m)			
	$\mathbf{d}_f$ added at 150s		$\mathbf{d}_f$ removed at 300s	
	Tendon controller	Linear controller	Tendon controller	Linear controller
30	29.06	32.36	5.57	0.07
100	**55.04**	76.05	**55.03**	**-43.91**
-30	5.37	0.08	28.95	32.36
-100	1.04	**-44.07**	**32.08**	75.97

∗ The vehicles undesired spacings are highlighted in bold. Negative values show the vehicles's collision and the communication lost is represented by bold positive value.

VI. Formation Maintenance and Manoeuvring

In this section, the overall formation system is described as a combination of tendon-driven systems outlined previously. The formation manoeuvring will be described and demonstrated through simulations.

A. Formation control and dynamic shape changes

In order to adapt to the changes in the environment such as obstacles, the formation control method should be flexible so that shape changes can be conveniently carried out. Here, formation control is achieved by maintaining the distances between nominated pairs of vehicles using the concept of tendon-driven system. Note that each vehicle in the formation is assumed to be autonomous and that it makes decisions based on the relative distance and bearing among individuals. For example, UV_2 makes its decision to move according to the distance (d_1) and relative orientation (θ_{ro1}) with respect to its leader, UV_1 as shown in Figure 9. The topology of closed-loop formation system composed of r communication links is depicted in Figure 10.

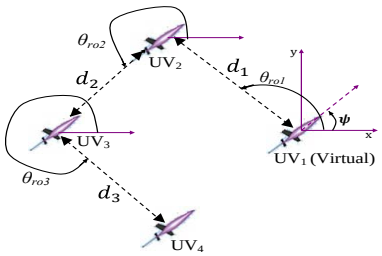

Figure 9: Relative parameters in formation

The synchronisation of two vehicles requires the consideration of the following equations:

$$\begin{aligned} x_{n+1} &= d_n \cos(\theta_{ron} + \psi) + x_n \\ y_{n+1} &= d_n \sin(\theta_{ron} + \psi) + y_n \end{aligned} \tag{10}$$

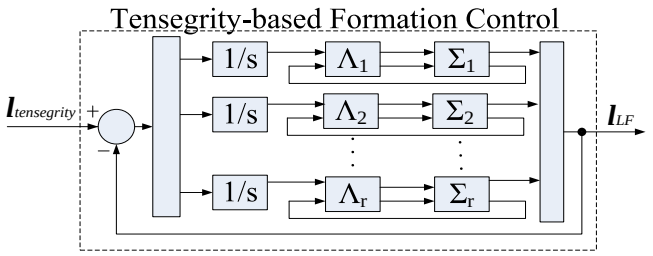

Figure 10: Block diagram of tensegrity-based formation closed-loop system. Tendon-driven systems and tendon controllers are denoted by Σ and Λ, respectively.

where $(x_{n+1},\ y_{n+1})$ is the updated relative position of UV_{n+1} and $(x_n,\ y_n)$ is the current position of its leader, UV_n in the global reference frame of coordinates. For formation shape change, vehicle's relative orientation (θ_{ron}) and the equilibrium spacing (d_n=$l_{tensegrity}$) along the edges are set as reference parameters. By controlling these variables, the shape changing task can be achieved.

B. Autopilot design

In order to design the controller, it is assumed that all the vehicles in the formation have the same dynamics which can be represented by a linear first order Nomoto model given by Equation 11.

$$T\ddot{\psi} + \dot{\psi} = K_n \delta \tag{11}$$

whose transfer function is:

$$\frac{\psi}{\delta}(s) = \frac{K_n}{s(1+Ts)} \tag{12}$$

Where K_n is the gain and T is the system time constant that can be uniquely determined from the input rudder angle (δ) and the output heading angle (ψ). From [12], the values of K_n and T are chosen to be 0.049 and 17.78 for simulation purposes.

An autopilot must have the function of maintaining the trajectory of the vehicle by following the desired heading (ψ(t)). It must also have the function of performing the change of heading without excessive oscillations and in the minimum possible time. In order to accomplish this, a suitable PD heading controller was developed which was tuned heuristically using trial and error.

The completed formation control setup is shown in Figure 11, where $\mathbf{q}$ is the position vector of the unmanned vehicle. The task was to move the leader with heading angle, ψ and velocity, v from one way-point to the next.

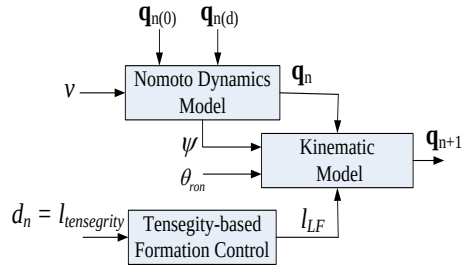

Figure 11: Block diagram of the formation control model

C. Simulation results

The tensegrity-based formation control design method was simulated using a group of four UVs in a diamond shape formation, as in Figure 9, where UV_1 is the virtual vehicle. The objectives were to regulate the inter-UV distances within the prescribed communications range and to perform the formation changing and manoeuvring tasks. Commanded and actual trajectories of the formation along the $x-$ and $y-$axis are shown in Figure 12. The formation was required to move from initial way-point (WP0) to the final waypoint (WP4), through WP1, WP2 and WP3 by following the line of sight (LOS) between successive waypoints. Note that there is no crossover or collisions between any of the vehicle's paths. However, a longer route was taken during turning manoeuvres due to constant velocity assumption in order to maintain the shape of the formation.

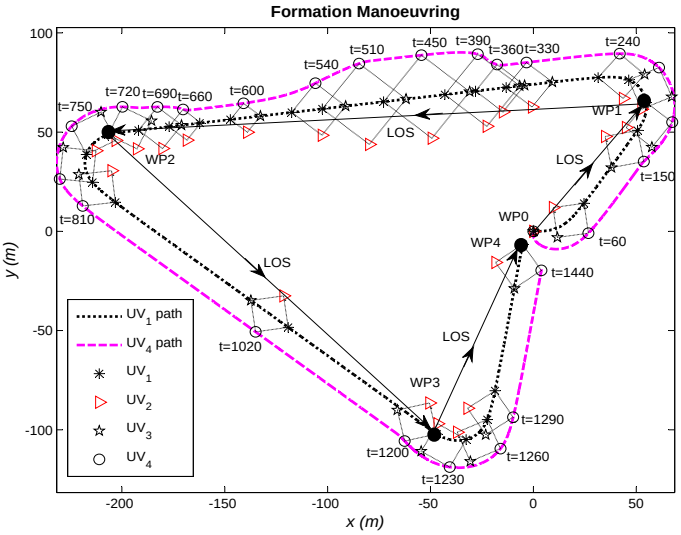

Figure 12: Simulations of formation changing and manoeuvring

The formation's size was changed twice at 350s and 500s for a period of 150s. In order to avoid any sudden changes to the formation and have to avoid inter-vehicle collisions, the reference input ($l_{tensegrity}$) in Figure 10 is taken to be a ramp signal with 0.5 slope. From the controller responses shown in Figure 13, it can be seen that the vehicles experience negative/repelling force when the shape dilation (parameter of d_n or $l_{tensegrity}$ was changed from 16m to 30m) is performed. The subsequent positive force is expected as in Figure 7. Note that a time frame of 30s is needed for this shape dilation task. A positive/attracting force was applied at time 500s to contract the quadrilaterals shape from edge length of 30m to 10m. A longer time (40s) is required for this task due to the nonlinear controller characteristics. The formation was returned to its original shape ($d_r = 16$m) at 650s with a negative force.

VII. Conclusions

A nonlinear control law that is modelled by the tendon-driven system using the concept of tensegrity structures is presented. It has been demonstrated that this control method

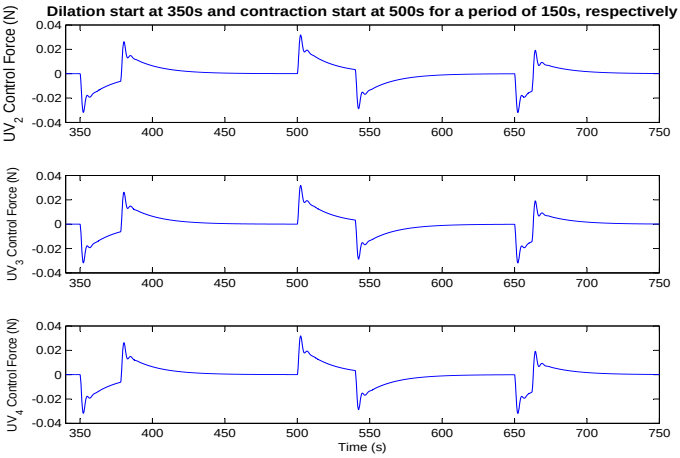

Figure 13: Simulations of input forces

can regulate the shape of formation in the presence of disturbances. The proposed approach is also scalable to any number of autonomous vehicles in the formation and is only limited by the communication bandwidth. It is also shown that the shape of the formation is conserved during manoeuvring. The shape changing algorithm can also be modified to include obstacle avoidance. Further research is required to develop more advanced mathematical machinery that can be used to analyse the stability of shape formation based on the tensegrity structures. The management of vehicle failures will also be considered in the future research.

References

[1] Y. Chen and Z. Wang, "Formation control: a review and a new consideration," in *Proceedings of IEEE/RSJ International Conference on Intelligent Robots and Systems*, Edmonton, Canada, 2-6 August 2005, pp. 3181 – 3186.

[2] Y. Esin and M. Ünel, "Formation control of nonholonomic mobile robots using implicit polynomials and elliptic fourier descriptors," *Turkish Journal of Electrical Engineering and Computer Sciences*, vol. 18, no. 5, pp. 765–780, 2010.

[3] M. Defoot, T. Floquet, A. Kökösy, and W. Perruquetti, "Sliding-mode formation control for cooperative autonomous mobile robots," *IEEE Transactions on Industrial Electronics*, vol. 55, no. 11, pp. 3944–3953, 2008.

[4] G. Mariottini, F. Morbidi, D. Prattichizzo, N. Valk, N. Michael, G. Pappas, and K. Daniilidis, "Vision-based localization for leader-follower formation control," *IEEE Transcation on Robotics*, vol. 25, no. 6, pp. 1431–1438, 2009.

[5] X. Li and J. Xiao, "Formation control in leader-follower motion using direct Lyapunov method," *International Journal of Intelligent Control and Systems*, vol. 10, no. 3, pp. 244–250, 2005.

[6] R. Skelton and M. Oliveira, *Tensegrity Systems*. New York: Springer, 2009, vol. XIV.

[7] B. Nabet and N. Leonard. (2009) Tensegrity models and shape control of vehicle formations. [Online]. Available: http://arxiv.org/pdf/0902.3710v1.pdf [Date accessed: 21 March 2012].

[8] K. Snelson, "Continuous tension, discontinuous compression structures," *U.S. Patent 3, 169, 611*, 1965.

[9] R. Fuller, "Tensile-integrity structures," *U.S. Patent 3, 063, 521*, 1962.

[10] R. Connelly, "Rigidity and energy," *Inventiones Mathematicae*, vol. 66, pp. 11–33, 1982.

[11] J. Aldrich, "Control synthesis for a class of light and agile robotic, tensegrity structures," Ph.D. dissertation, Department of Mechanical and Aerospace Engineering, University of California, San Diego, 2004.

[12] C. Tzeng and J. Chen, "Fundamental properties of linear ship steering dynamic models," *Journal of Marine Science and Technology*, vol. 7, no. 2, pp. 78–88, 1999.